# Integrated Proteomic and miRNA Transcriptional Analysis Reveals the Hepatotoxicity Mechanism of PFNA Exposure in Mice

**ARTICLE** *in* JOURNAL OF PROTEOME RESEARCH · SEPTEMBER 2014

Impact Factor: 4.25 · DOI: 10.1021/pr500641b · Source: PubMed



**5 AUTHORS**, INCLUDING:

Jianshe Wang
Chinese Academy of Sciences
**38** PUBLICATIONS **654** CITATIONS
SEE PROFILE

Shengmin Yan
Indiana University-Purdue University Indiana…
**7** PUBLICATIONS **24** CITATIONS
SEE PROFILE

Hongxia Zhang
Lanzhou University
**48** PUBLICATIONS **784** CITATIONS
SEE PROFILE

Jiayin Dai
Chinese Academy of Sciences
**94** PUBLICATIONS **1,907** CITATIONS
SEE PROFILE

Journal of proteome research

Article

pubs.acs.org/jpr

# Integrated Proteomic and miRNA Transcriptional Analysis Reveals the Hepatotoxicity Mechanism of PFNA Exposure in Mice

Jianshe Wang, Shengmin Yan, Wei Zhang, Hongxia Zhang, and Jiayin Dai*

Key Laboratory of Animal Ecology and Conservation Biology, Institute of Zoology, Chinese Academy of Sciences, Beijing 100101, People's Republic of China

Supporting Information

**ABSTRACT:** Perfluoroalkyl chemicals (PFASs) are a class of highly stable man-made compounds, and their toxicological impacts are currently of worldwide concern. Administration of perfluorononanoic acid (PFNA), a perfluorocarboxylic acid (PFCA) with a nine carbon backbone, resulted in dose-dependent hepatomegaly in mice (0, 0.2, 1, and 5 mg/kg body weight, once a day for 14 days) and an increase in hepatic triglycerides (TG) and total cholesterol (TCHO) in the median dose group as well as serum transaminases in the high dose group. Using isobaric tags for relative and absolute quantitation (iTRAQ), we identified 108 (80 up-regulated, 28 down-regulated) and 342 hepatic proteins (179 up-regulated, 163 down-regulated) that exhibited statistically significant changes (at least a 1.2-fold alteration and $P < 0.05$) in the 1 and 5 mg/kg/d PFNA treatment groups, respectively. Sixty-six proteins (54 up-regulated, 12 down-regulated) significantly changed in both of the two treatment groups. Among these 54 up-regulated proteins, most were proteins related to the lipid metabolism process (31 proteins). The mRNA analysis results further suggested that PFNA exposure not only resulted in a fatty acid oxidation effect but also activated mouse liver genes involved in fatty acid and cholesterol synthesis. Additionally, three (2 down-regulated, 1 up-regulated) and 30 (14 down-regulated, 16 up-regulated) microRNAs (miRNAs) exhibited at least a 2-fold alteration ($P < 0.05$) in the 1 and 5 mg/kg/d PFNA treatment groups, respectively, Three miRNAs (up-regulated: miR-34a; down-regulated: miR-362-3p and miR-338-3p) significantly changed in both of the two treatment groups. The repression effect of miR-34a on fucosyltransferase 8 (Fut8) and lactate dehydrogenase (Ldha) was confirmed by luciferase activity assay and Western blot analysis. The results implied that PFNA exerted a hepatic effect, at least partially, by miRNAs mediated post-translational protein repression.

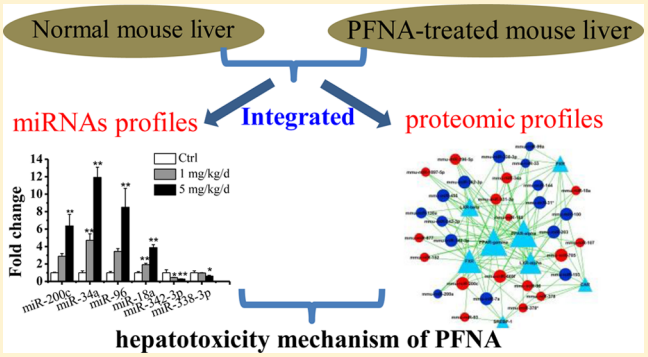


**KEYWORDS:** *PFNA, miRNAs, iTRAQ, hepatotoxicity*

## INTRODUCTION

Perfluoroalkyl substances (PFASs) are man-made compounds consisting of fluorinated carbon backbones of varying length and are widely used in industrial and consumer products.[1] They are characterized by carbon-fluoride bonds that allow them to be highly stable and, therefore, environmentally persistent. PFASs are also widespread, with reports showing that PFASs are existent in human populations, wildlife, and environmental matrices.[2−6] Among all PFASs, eight-carbon-chain perfluorooctanesulfonate (PFOS) and perfluorooctanoic acid (PFOA) are among the most widely detected and studied. Since 2000, the emission of PFOS and PFOA have decreased due to changes in the manufacturing practice for them.[7] However, hundreds of related chemicals with shorter or longer alkyl chains remain unregulated and continue to be released into the environment.[8,9] For example, perfluorononanoic acid (PFNA), a perfluorocarboxylic acid (PFCA) with a nine-carbon backbone, has been detected throughout the world in human blood and animal tissue and research has shown that the mean concentration of PFNA levels in both mediums have been continually increasing.[10,11]

PFASs are both lipo- and hydrophobic, and after absorption, they will bind to proteins in serum and the liver rather than accumulating in lipid.[12,13] Moreover, studies suggest that exposure to PFASs (PFOA and possibly PFOS) may be associated with increased total cholesterol (TCHO), low-density lipoprotein cholesterol (LDL-C), and triglycerides (TG) in humans.[2,14,15] In laboratory animals, loss of body weight, tumorigenicity, and many other toxicological hazards have been observed after PFAS exposure.[7,16,17] Laboratory animal studies have also indicated that some PFASs induce toxicological hazards via a PPAR $\alpha$ agonistic mode in rodents,[17,18] and other pathways may also be involved.[19] MicroRNA (miRNA) is a type of endogenous, small noncoding

**Special Issue:** Environmental Impact on Health

**Received:** June 25, 2014

   dx.doi.org/10.1021/pr500641b | J. Proteome Res. XXXX, XXX, XXX−XXX

RNA which regulates gene expression by base-pairing to complementary sites on target mRNAs to block translation or trigger their degradation.[20] Although many studies have shown aberrant miRNA expression in diseases,[21] little is known regarding whether environmental pollutants can induce such changes. This paper hypothesizes that PFNA exposure may also lead to disruption of normal miRNA expression patterns, which represents a plausible novel pathway capable of explaining the hepatic effect of this chemical.

Proteomics is a powerful method that provides insight into the mechanisms of toxic compounds[22] and isobaric tags for relative and absolute quantitation (iTRAQ) is a popular proteomic method[23] that can be used for multiplexed protein profiling of up to eight different samples during a single experiment. In this study, by combining eight-plex iTRAQ reagent labeling followed by high-performance liquid chromatography-tandem mass spectrometry (HPLC−MS/MS) with miRNA expression profile analysis, we aimed to (a) gain insight into the effects of PFNA on livers and (b) explore the hepatic miRNA response to PFNA exposure as well as the potential role of miRNAs with altered expression levels in response to hepatic effects induced by PFNA.

## MATERIALS AND METHODS

### Chemicals and Animals

PFNA was obtained from Sigma-Aldrich (St. Louis, MO, U.S.A.) (CAS number 375-95-1, 97% purity). Male BALB/c mice at 6−8 weeks of age were purchased from Weitong Lihua Experimentary Animal Central (Beijing, China) and maintained in a mass air-displacement room with a 12-h light-dark cycle at a temperature of 20−26 °C and a relative humidity of 50−70%. After 1 week of acclimatization, the mice were randomly separated into four groups ($n$ = 8 per group) and treated with PFNA (0, 0.2, 1, and 5 mg/kg body weight, respectively) via gastric gavage once a day for 14 days. At the end of the experiment, all animals were sacrificed by cervical dislocation. Livers were removed, weighed, cut into small pieces, and then frozen in liquid nitrogen immediately and stored at −80 °C for PFNA analysis, RNA and protein extraction. Blood was collected, placed at room temperature to coagulate, and then centrifuged at 2000$g$ for 15 min. Serum was stored at −80 °C until analysis. All experimental manipulations were undertaken according to protocols approved by the Animal Ethics Committee of the Institute of Zoology (IOZ), Chinese Academy of Sciences (CAS).

### PFNA Content, Serum Parameters, and Hepatic Lipids Analysis

The PFNA contents in liver and serum samples were quantified using HPLC−MS/MS. Detailed information for PFNA content detection as well as quality control are given in the Supporting Information Methods and Table S1. Standard spectrophotometric methods for the Hitachi7170A automatic analyzer were used to measure serum parameters, including TG, TCHO, alanine transaminase (ALT), and aspartate aminotransferase (AST). Partial hepatic samples were finely minced and extracted overnight at 4 °C in 1 mL of $n$-heptane:dimethylcarbinol (2:3.5), Extractable lipid content was measured using a commercially available kit (Biosino Biotechnology and Science Inc., Beijing, China).

### mRNA Quantitative PCR (qPCR)

We used qPCR to analyze mRNA alteration of lipid metabolism-related genes after PFNA treatment. Total RNA was isolated from frozen mice liver using Trizol reagent (Invitrogen, Carlsbad, CA, U.S.A.). Yield and quality of RNA were routinely assessed using ultraviolet absorbance and electrophoresis. The cDNA was synthesized from hepatic total RNA using oligo-$(dT)_{15}$ primer (Promega, Madison, WI, U.S.A.) and M-MuLV reverse transcriptase (New England Biolabs, Hitchin, U.K.). The cDNA was then used as a template in 25 $\mu$L reactions containing 12.5 $\mu$L of 2 × QuantiTect SYBR Green PCR master mix and 0.1 $\mu$M each of forward and reverse gene-specific primers. Glyceraldehyde-3-phosphate dehydrogenase (Gapdh) was chosen as the internal control for normalization. Primer information is listed in Supporting Information Table S2. The qPCR reactions were performed with the Stratagene Mx3000P qPCR system (Stratagene, La Jolla, CA, U.S.A.) under the following conditions: denaturing at 95 °C for 2 min followed by 40 cycles of 15 s at 95 °C, 15 s at 58 °C, and 15 s at 72 °C. Melting curve analysis (60−95 °C) and gel electrophoresis were used for assessing amplification specificity. For each qPCR assay, at least six individuals in each group were used, and the means and SE were derived from these biological samples. Relative abundance of each mRNA was calculated using the $2^{-\Delta\Delta CT}$ method.[24] One-way ANOVA followed by Fisher's least significant difference test were conducted for statistical analysis using SPSS for windows v14.0 (SPSS, Inc., Chicago, IL, U.S.A.), with $P < 0.05$ considered significant.

### iTRAQ Labeling and Protein Digestion

Based on the results regarding hepatic lipids and serum transaminases, the control and the 1 and 5 mg/kg body weight PFNA exposure groups were selected for further proteomics analysis. Liver tissues from two individual animals in the same group were pooled, and totally eight animals in each group were used. Therefore, each group prepared for iTRAQ labeling consisted of four pooled samples.

For each sample, proteins were precipitated using ice-cold acetone and then were redissolved in dissolution buffer (0.5 M triethylammonium bicarbonate, 0.1% SDS). Next, proteins were quantified using the bicinchoninic acid method, 100 $\mu$g of protein was tryptically digested, and the resultant peptide mixture was labeled using iTRAQ reagent (Applied Biosystems, California, U.S.A.). Disulfide bonds were reduced in 5 mM Tris(2-carboxyethy) phosphine (TCEP) for 1 h at 60 °C, followed by blocking cysteine residues in 10 mM methylmethanethiosulfonate (MMTS) for 30 min at room temperature before undergoing digestion using sequence-grade modified trypsin (Promega, Madison, WI, U.S.A). For labeling, each iTRAQ reagent was dissolved in 50 $\mu$L of isopropanol and added to the respective peptide mixture. Proteins were labeled with the iTRAQ tags as following: Samples in the control group were labeled with the 113, 114, 115, and 116 isobaric tag; samples in the 1 mg/kg/d PFNA treatment group were labeled with the 117, 118, 119, and 121 isobaric tag; samples in the 5 mg/kg/d PFNA treatment group were also labeled with the 117, 118, 119, and 121 isobaric tag. The labeled samples were combined (One combination was made between the control and the 1 mg/kg/d PFNA treatment group. Another combination consisted of the control and the 5 mg/kg/d PFNA treatment group) and dried in vacuum.


dx.doi.org/10.1021/pr500641b | J. Proteome Res. XXXX, XXX, XXX−XXX

### High pH Reversed Phase Separation

The peptide mixture was redissolved in buffer A (buffer A: 20 mM ammonium formate in water, pH 10.0, adjusted with ammonium hydroxide) and then fractionated by high pH separation using a Aquity UPLC system (Waters Corporation, Milford, MA) connected to a reverse phase column (XBridge C18 column, 2.1 mm × 150 mm, 3.5 μm, 300 Å, Waters Corporation, Milford, MA). High pH separation was performed using a linear gradient. Starting from 5% B to 35% B in 40 min (B: 20 mM ammonium formate in 90% ACN, pH 10.0, adjusted with ammonium hydroxide), the column was re-equilibrated at initial conditions for 15 min. The column flow rate was maintained at 200 μL/min and column temperature was maintained at room temperature. Seven fractions were collected and each fraction was dried in a vacuum concentrator for the next step.

### Low pH Nano-HPLC–MS/MS Analysis

The peptides were resuspended with 20 μL of solvent C (C: water with 0.1% formic acid; D: ACN with 0.1% formic acid) and separated by nanoLC, then were analyzed by online electrospray tandem mass spectrometry. The experiments were performed using a Nano Aquity UPLC system (Waters Corporation, Milford, MA, U.S.A.) connected to a Q Exactive hybrid quadrupole-Orbitrap mass spectrometer (Thermo Fisher Scientific, San Jose, CA, U.S.A.) equipped with an online nanoelectrospray ion source. Each time (replicated twice) 8 μL of the peptide sample was loaded onto a Thermo Scientific Acclaim PepMap C18 column (100 μm × 2 cm, 3 μm particle size) with a flow of 10 μL/min for 3 min and then subsequently separated on the analytical column (Acclaim PepMap C18, 75 μm × 15 cm) with a linear gradient, from 5% D to 45% D in 105 min. The column was re-equilibrated at initial conditions for 15 min. The column flow rate was maintained at 300 nL/min and column temperature was maintained at 40 °C. The electrospray voltage of 1.9 kV versus the inlet of the mass spectrometer was used.

Q Exactive mass spectrometer was operated using the data-dependent mode to switch automatically between MS and MS/MS acquisition. Survey full-scan MS spectra ($m/z$ 400–1800) were acquired with a mass resolution of 70 K, followed by 10 sequential high energy collisional dissociation (HCD) MS/MS scans with a resolution of 17.5 K. In all cases, one microscan was recorded using a dynamic exclusion of 30 s. MS/MS fixed first mass was set at 100.

### Database Searching and Criteria

Thermo Scientific Proteome Discoverer software version 1.4 with the MASCOT v2.3.2 search engine was used for all database searches. The database chosen was the Mouse UniProtKB/Swiss-Prot database (Release 2012-12-27, with 16 409 sequences). Raw files generated by the Q Exactive instrument were searched directly using 10 ppm precursor mass tolerance and 20 mmu fragment mass tolerance. The enzyme specificity with trypsin was used. Up to two missed cleavages were allowed and peptides with at least seven amino acids were retained. Methylthio of cysteines, iTRAQ modification of peptide N-termini and lysine residues were set as fixed modifications and methionine oxidation was set as the variable modification. Identification quality control: The target-decoy based strategy was applied to control peptide level false discovery rates (FDR) lower than 1%. Only unique peptides were used for protein quantification, and the method of normalization on protein median was used to correct experimental bias. Also, the minimum number of proteins that must be observed to allow was set to 1000.

To identify the differentially expressed proteins by PFNA treatment, protein changed levels were compared between the treatment group (1 or 5 mg/kg/d of PFNA) and the control using Student's $t$-test. Setting the FDR level to 0.1, we controlled the FDR with Benjamini and Hochberg's procedure.[25] There were duplicated technical repeats in each HPLC–MS/MS experiment, and proteins were considered up- or down-regulated when their ratios were ≥1.2 or ≤0.83 ($P < 0.05$) in the treatment group compared with that in the control in both of the duplicated technical repeats. The changed proteins were sorted according to their biological functions by searching Gene Ontology (GO) (http://www.geneontology.org).

### MiRNA Level Analysis

The control and the 1 and 5 mg/kg body weight PFNA exposure groups were selected for further miRNA level detection. Liver tissue from two individual mice in the same group were pooled into one sample, and the hepatic total RNA from three pooled samples in each group were labeled and hybridized with mouse miRNA arrays (Agilent Technologies, Santa Clara, CA, U.S.A.), which contained probes for 627 mouse miRNAs and 39 mouse viral microRNAs based on Sanger miRBase v12.0 according to the manufacturer's protocols. Microarray results were extracted using Agilent Feature Extraction Software and analyzed using GeneSpring GX (Agilent Technologies, Santa Clara, CA, U.S.A.). To obtain miRNAs that were significantly changed by PFNA treatment, a 2-fold and $P < 0.05$ threshold was set. To further confirm the microarray data, six miRNAs (miR-34a, miR-200c, miR-96, miR-18a, miR-338-3p, and miR-342-3p), which were significantly altered by high PFNA dose and whose sequences are conserved between rodents and human, were selected for TaqMan qPCR analysis. The cDNA was synthesized from mice hepatic total RNA samples using specific miRNA primers from the TaqMan microRNA assays and reagents from the TaqMan microRNA reverse transcription kit. The PCR products were amplified using the TaqMan MicroRNA Assay together with the TaqMan Universal PCR Master Mix. The TaqMan MicroRNA Assay for U6 snRNA, which was not changed in the miRNA array after PFNA treatment, was used as the internal control for normalization. All reverse transcription and PCR reactions were performed according the manufacturer's protocols. The same method as mRNA qPCR was used for fold change calculation and statistical analysis. Searching potential targets of altered miRNAs from the altered proteins by iTRAQ assay was carried out using the online database StarBase 2.0 (http://starbase.sysu.edu.cn/), which can explore microRNA–mRNA interaction maps from cross-linking and Argonaute immunoprecipitation coupled with high-throughput sequencing (CLIP-Seq) data, combined with miRNA target prediction programs: PicTar, TargetScan, RNA22, PITA, and miRanda.[26,27]

### Plasmid Preparation, Transfection and Confirmation of miRNA Targets

The relevant 3′ UTR sequences in lactate dehydrogenase A (Ldha) and fucosyltransferase 8 (Fut8), which contained the putative target site for miR-34a, were amplified from mice genomic DNA (detailed primer information is shown in Supporting Information Table S3) inserted into the psiCHECK-2 vector (Promega, Madison, WI, U.S.A.) and


dx.doi.org/10.1021/pr500641b | J. Proteome Res. XXXX, XXX, XXX–XXX

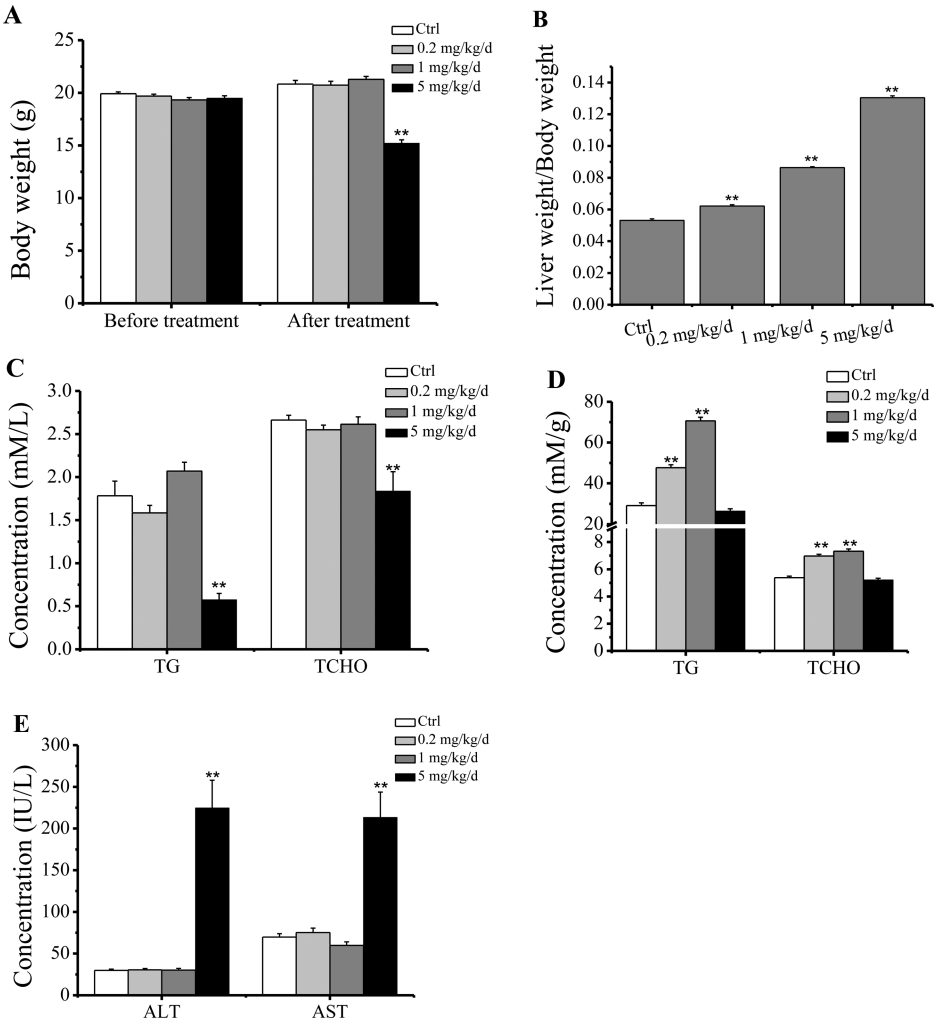


**Figure 1.** Mice phenotypes after PFNA exposure. BALB/c mice were treated with 0, 0.2, 1, and 5 mg/kg/d PFNA for 14 days. (A) Body weights before and after treatment. (B) Liver weight after treatment. (C) Serum triglyceride (TG) and total cholesterol (TCHO) concentrations. (D) Liver TG and TCHO concentrations. (E) Serum alanine transaminase (ALT) and aspartate aminotransferase (AST) levels. Differences were evaluated using one-way ANOVA followed by Fisher's least significant difference test. Error bars represent standard error (SE) ($n = 6$). * $P < 0.05$ versus Ctrl, ** $P < 0.01$ versus Ctrl.

then confirmed by sequencing (named psiCHECK-Ldha and psiCHECK-Fut8, respectively).

The HepG2 cells (ATCC No. HB-8065) were maintained at 37 °C in Dulbecco's Modified Eagle's Medium (DMEM) (Gibco, Invitrogen, Carlsbad, CA, U.S.A.) supplemented with 10% fetal bovine serum (FBS) (Hyclone Laboratories, Logan, UT, U.S.A.). To mimic the increase in miR-34a and detect the response of their candidate target genes, HepG2 cells ($2.5 \times 10^5$) plated in a 24-well plate were cotransfected with miR-34a mimics (Dharmacon Research Inc., Lafayette, CO, U.S.A.; 25 nM final concentration) and 1 $\mu$g of target reporter plasmid (psiCHECK-Ldha or psiCHECK-Fut8) using Lipofectamine 2000 (Invitrogen, Carlsbad, CA, U.S.A.) according to the manufacturer's instructions. After 48 h post-transfection, cells were collected for qPCR, Western blotting, and luciferase activity assays. For qPCR, the same method as lipid metabolism-related genes was used. The primers used are listed in Supporting Information Table S2. For Western blot analysis, 60 $\mu$g of the protein extract was separated on 10% SDS-PAGE gels and then electrophoretically transferred to a PVDF membrane (PALL, Ann Arbor, MI, U.S.A.). The membrane was blocked in freshly prepared TBST buffer (25 mM Tris-HCl pH 7.5, 150 mM NaCl and 0.1% Tween-20) containing 5% nonfat dry milk for 1 h at room temperature. Blots were incubated with rabbit polyclonal antibodies of Ldha (Abcam, Cambridge, MA, U.S.A.) and Fut8 (Santa Cruz Biotechnology, Delaware Avenue, CA, U.S.A.) at a 1:500 dilution. $\beta$-Actin (Santa Cruz Biotechnology, Delaware Avenue, CA, U.S.A.) or $\beta$-tubulin antibodies (Santa Cruz Biotechnology, Delaware Avenue, CA, U.S.A.) diluted at 1:2000 were used to normalize the amount of proteins. The membranes were then rinsed three times with TBST, each for 10 min, incubated with peroxidase-conjugated goat antirabbit IgG (Santa Cruz Biotechnology, Delaware Avenue, CA, U.S.A.) for 1 h at room temperature, and then washed for another 30 min with TBST buffer. Band detection was performed using the LumiGLO chemiluminescent substrate kit (CST, Beverly, MA, U.S.A.) according to manufacturer's instructions. AlphaImager 2200 (Alpha-InnoTec Corporation, San Leandro, CA, U.S.A.) software was used to determine the density of the protein bands. Firefly and Renilla luciferase activity assays were conducted using the standard Dual-Luciferase Reporter Assay System (Promega, Madison, WI, U.S.A.) according to the manufacturer's instructions. Relative protein levels were


dx.doi.org/10.1021/pr500641b | J. Proteome Res. XXXX, XXX, XXX−XXX

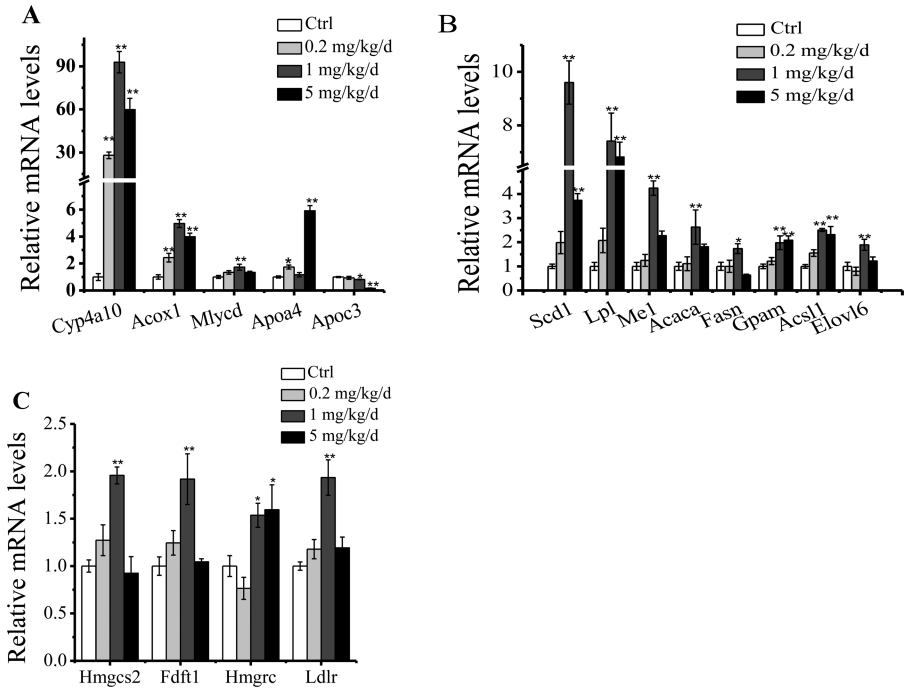


**Figure 2.** Hepatic mRNA levels of lipid and cholesterol metabolism-related genes. (A) mRNA levels of PPAR $\alpha$ target genes. Apolipoprotein A-IV (Apoa4), acyl-Coenzyme A oxidase 1, palmitoyl (Acox1), malonyl-CoA decarboxylase (Mlycd), cytochrome P450, family 4, subfamily a, polypeptide 10 (Cyp4a10), and apolipoprotein C−III (Apoc3). (B) mRNA levels of SREBP-responsive genes in fatty acid metabolism and plasma lipoprotein metabolism pathways. Fatty acid synthase (Fasn), acetyl-Coenzyme A carboxylase $\alpha$ (Acaca), acyl-CoA synthetase long-chain family member 1 (Acsl1), malic enzyme 1, NADP(+)-dependent, cytosolic (Me1), stearoyl-Coenzyme A desaturase 1 (Scd1), ELOVL family member 6, elongation of long chain fatty acids (Elovl6), glycerol-3-phosphate acyltransferase, mitochondrial (Gpam), and lipoprotein lipase (Lpl). (C) mRNA levels of SREBP target genes in the cholesterol biosynthetic pathway. Low density lipoprotein receptor (Ldlr), 3-hydroxy-3-methylglutaryl Coenzyme A reductase (Hmgcr), 3-hydroxy-3-methylglutaryl Coenzyme A synthase 2 (Hmgcs2), and farnesyl-diphosphate farnesyltransferase 1 (Fdft1). Gapdh was chosen as an internal control for normalization. Differences were evaluated using one-way ANOVA followed by Fisher's least significant difference test. Error bars represent standard error (SE) ($n$ = 6). * $P$ < 0.05 versus control, ** $P$ < 0.01 versus control.

expressed as Renilla/firefly luciferase ratios. Student's $t$-test was used to evaluate the differences between groups in the above assays.

## RESULTS

### PFNA Contents and Classic End Points after PFNA Treatment

The content of PFNA in the mice livers and serum after 2 weeks of exposure were quantified by HPLC−MS/MS. The hepatic content of PFNA was higher than that in serum at the same exposure dose, with liver content of 24.3, 46.9, and 172.3 $\mu$g/g and serum content of 11.5, 38.5, and 156.1 $\mu$g/mL in the 0.2, 1, and 5 mg/kg/d PFNA treatment groups, respectively (Supporting Information Figure S1A and S1B). After PFNA treatment, though no significant changes were observed in the other two treatment groups, the highest PFNA dose (5 mg/kg/d) treated mice showed a significant decrease in body weight compared with the control group (Figure 1A). Liver weight was a more sensitive parameter to PFNA, with the hepato/somatic index (ratio of liver weight to body weight) increasing by 17% even in the low dose group (Figure 1B). Serum TG and TCHO decreased significantly in the 5 mg/kg/d PFNA treatment group (Figure 1C). However, TG and TCHO levels in liver homogenate significantly increased in both the 0.2 and 1 mg/kg/d PFNA treatment groups compared with the control ($P$ < 0.05), and no detectable alterations were observed in livers from the highest PFNA dose treatment (Figure 1D). Serum ALT and AST, two transaminases that leak into the bloodstream when liver cells are damaged, increased in the highest dose group compared with the control (Figure 1E).

### Effect of PFNA on Hepatic Lipid Metabolism Pathways

Peroxisome proliferator-activated receptors $\alpha$ (PPAR $\alpha$) and sterol regulatory element-binding proteins (SREBPs) are the key transcription regulators of genes involved in fatty acid oxidation and lipid biosynthesis reaction, respectively. To confirm the effect of PFNA on lipid metabolism, the hepatic mRNA levels of PPAR $\alpha$ and SREBP target genes after PFNA treatment were detected using qPCR. The hepatic mRNA levels of PPAR $\alpha$ targets peroxisomal acyl-coenzyme A oxidase 1 (Acox1), cytochrome P450 4A10 (Cyp4a10), apolipoprotein A-IV (Apoa4), and malonyl-CoA decarboxylase (Mlycd) showed an increased tendency in PFNA-treated livers compared with the control, with at least one treatment group increased significantly. Conversely, the hepatic mRNA level of apolipoprotein C-III (Apoc3), which was negatively regulated by PPAR $\alpha$, decreased in the PFNA treatment groups (Figure 2A). The mRNA levels of SREBP-responsive genes involved in the fatty acid metabolism pathway were all up-regulated in the hepatic tissue of mice exposed to 1 mg/kg/d PFNA for 14 days, including long-chain-fatty-acid-CoA ligase 1 (Acsl1), stearoyl-Coenzyme A desaturase 1 (Scd1), NADP-dependent malic enzyme (Me1), acetyl-Coenzyme A carboxylase $\alpha$ (Acaca), fatty acid synthase (Fasn), glycerol-3-phosphate acyltransferase, mitochondrial (Gpam), ELOVL family member 6, elongation of long chain fatty acids (Elovl6), and genes in the plasma lipoprotein metabolism pathway, such as lipoprotein lipase


dx.doi.org/10.1021/pr500641b | J. Proteome Res. XXXX, XXX, XXX−XXX

**Table 1. Significantly Changed Proteins in Both 1 and 5 mg/kg/d PFNA Treatment Groups[a]**

| | | | 1 mg/kg/d versus Ctrl | | 5 mg/kg/d versus Ctrl | |
|---|---|---|---|---|---|---|
| accession | gene name | protein name | fold change | *P* value | fold change | *P* value |
| | | Up-Regulated | | | | |
| Q9DD20 | Mettl7b | Methyltransferase-like protein 7B [MET7B] | 1.21 | 0.0011 | 1.83 | 0.0000 |
| P24270 | Cat | Catalase [CATA] | 1.22 | 0.0000 | 1.24 | 0.0003 |
| O35678 | Mgll | Monoglyceride lipase [MGLL] | 1.23 | 0.0001 | 1.24 | 0.0014 |
| O08601 | Mttp | Microsomal triglyceride transfer protein large subunit [MTP] | 1.23 | 0.0001 | 1.38 | 0.0000 |
| Q9WV68 | Decr2 | Peroxisomal 2,4-dienoyl-CoA reductase [DECR2] | 1.24 | 0.0000 | 1.44 | 0.0001 |
| P24549 | Aldh1a1 | Retinal dehydrogenase 1 [AL1A1] | 1.25 | 0.0005 | 1.27 | 0.0099 |
| P51660 | Hsd17b4 | Peroxisomal multifunctional enzyme type 2 [DHB4] | 1.25 | 0.0001 | 1.56 | 0.0001 |
| Q9R0M6 | Rab9a | Ras-related protein Rab-9A [RAB9A] | 1.26 | 0.0008 | 1.49 | 0.0001 |
| Q9QXE0 | Hacl1 | 2-hydroxyacyl-CoA 1 [HACL1] | 1.28 | 0.0000 | 1.31 | 0.0001 |
| Q9JM62 | Reep6 | Receptor expression-enhancing protein 6 [REEP6] | 1.28 | 0.0006 | 1.49 | 0.0022 |
| Q8BMS1 | Hadha | Trifunctional enzyme subunit $\alpha$, mitochondrial [ECHA] | 1.31 | 0.0000 | 1.34 | 0.0001 |
| Q91WL5 | Cyp4a12a | Cytochrome P450 4A12A [CP4CA] | 1.31 | 0.0015 | 1.37 | 0.0021 |
| Q9Z2G9 | Htatip2 | Oxidoreductase HTATIP2 [HTAI2] | 1.32 | 0.0055 | 1.74 | 0.0000 |
| Q99JY0 | Hadhb | Trifunctional enzyme subunit $\beta$, mitochondrial [ECHB] | 1.33 | 0.0001 | 1.49 | 0.0000 |
| P43883 | Plin2 | Perilipin-2 [PLIN2] | 1.33 | 0.0002 | 1.23 | 0.0136 |
| Q3UUI3 | Them4 | Thioesterase superfamily member 4 [THEM4] | 1.35 | 0.0005 | 1.37 | 0.0059 |
| Q8CC88 | Kiaa0564 | Uncharacterized protein KIAA0564 homologue [K0564] | 1.36 | 0.0000 | 1.48 | 0.0000 |
| Q9WUZ9 | Entpd5 | Ectonucleoside triphosphate diphosphohydrolase 5 [ENTP5] | 1.37 | 0.0001 | 1.41 | 0.0003 |
| P42125 | Eci1 | Enoyl-CoA delta isomerase 1, mitochondrial [ECI1] | 1.37 | 0.0001 | 1.56 | 0.0001 |
| P34914 | Ephx2 | Epoxide hydrolase 2 [HYES] | 1.37 | 0.0000 | 1.53 | 0.0004 |
| P54869 | Hmgcs2 | Hydroxymethylglutaryl-CoA synthase, mitochondrial [HMCS2] | 1.37 | 0.0000 | 1.57 | 0.0000 |
| Q61133 | Gstt2 | Glutathione S-transferase theta-2 [GSTT2] | 1.38 | 0.0030 | 1.32 | 0.0002 |
| Q2TPA8 | Hsdl2 | Hydroxysteroid dehydrogenase-like protein 2 [HSDL2] | 1.39 | 0.0003 | 1.92 | 0.0000 |
| Q99LB2 | Dhrs4 | Dehydrogenase/reductase SDR family member 4 [DHRS4] | 1.40 | 0.0001 | 1.37 | 0.0000 |
| Q8BWN8 | Acot4 | Acyl-coenzyme A thioesterase 4 [ACOT4] | 1.41 | 0.0015 | 1.53 | 0.0002 |
| P58137 | Acot8 | Acyl-coenzyme A thioesterase 8 [ACOT8] | 1.43 | 0.0001 | 1.56 | 0.0001 |
| Q9CQ62 | Decr1 | 2,4-dienoyl-CoA reductase, mitochondrial [DECR] | 1.43 | 0.0000 | 1.48 | 0.0000 |
| Q80XL6 | Acad11 | Acyl-CoA dehydrogenase family member 11 [ACD11] | 1.43 | 0.0001 | 1.52 | 0.0000 |
| Q5FW57 | Gm4952 | Glycine N-acyltransferase-like protein [GLYAL] | 1.45 | 0.0000 | 1.64 | 0.0001 |
| P00493 | Hprt1 | Hypoxanthine-guanine phosphoribosyltransferase [HPRT] | 1.46 | 0.0001 | 1.62 | 0.0001 |
| Q921H8 | Acaa1a | 3-ketoacyl-CoA thiolase A, peroxisomal [THIKA] | 1.52 | 0.0012 | 1.64 | 0.0001 |
| P45952 | Acadm | Medium-chain specific acyl-CoA dehydrogenase, mitochondrial [ACADM] | 1.52 | 0.0000 | 1.74 | 0.0000 |
| P53808 | Pctp | Phosphatidylcholine transfer protein [PPCT] | 1.52 | 0.0026 | 1.60 | 0.0005 |
| P06801 | Me1 | NADP-dependent malic enzyme [MAOX] | 1.52 | 0.0000 | 1.31 | 0.0013 |
| Q9CYH2 | Fam213a | Redox-regulatory protein PAMM [PAMM] | 1.54 | 0.0000 | 1.35 | 0.0003 |
| P31786 | Dbi | Acyl-CoA-binding protein [ACBP] | 1.54 | 0.0000 | 1.21 | 0.0124 |
| Q8BIW1 | Prune | Protein prune homologue [PRUNE] | 1.56 | 0.0003 | 1.95 | 0.0002 |
| P55096 | Abcd3 | ATP-binding cassette subfamily D member 3 [ABCD3] | 1.56 | 0.0001 | 2.22 | 0.0019 |
| Q8JZR0 | Acsl5 | Long-chain-fatty-acid–CoA ligase 5 [ACSL5] | 1.56 | 0.0000 | 1.70 | 0.0000 |
| P12791 | Cyp2b10 | Cytochrome P450 2B10 [CP2BA] | 1.58 | 0.0001 | 1.52 | 0.0025 |
| Q08857 | Cd36 | Platelet glycoprotein 4 [CD36] | 1.60 | 0.0191 | 1.49 | 0.0012 |
| P12710 | Fabp1 | Fatty acid-binding protein, liver [FABPL] | 1.61 | 0.0000 | 1.40 | 0.0104 |
| P47934 | Crat | Carnitine O-acetyltransferase [CACP] | 1.62 | 0.0000 | 1.69 | 0.0001 |
| O88833 | Cyp4a10 | Cytochrome P450 4A10 [CP4AA] | 1.64 | 0.0000 | 2.08 | 0.0002 |
| O55137 | Acot1 | Acyl-coenzyme A thioesterase 1 [ACOT1] | 1.65 | 0.0002 | 1.61 | 0.0002 |
| P41216 | Acsl1 | Long-chain-fatty-acid–CoA ligase 1 [ACSL1] | 1.69 | 0.0000 | 1.95 | 0.0000 |
| Q9QYR9 | Acot2 | Acyl-coenzyme A thioesterase 2, mitochondrial [ACOT2] | 1.70 | 0.0001 | 2.06 | 0.0000 |
| Q9R0H0 | Acox1 | Peroxisomal acyl-coenzyme A oxidase 1 [ACOX1] | 1.74 | 0.0000 | 2.04 | 0.0000 |
| Q9EQ06 | Hsd17b11 | Estradiol 17-$\beta$-dehydrogenase 11 [DHB11] | 1.78 | 0.0075 | 1.61 | 0.0000 |
| P47740 | Aldh3a2 | Fatty aldehyde dehydrogenase [AL3A2] | 1.81 | 0.0000 | 2.16 | 0.0000 |
| Q9Z0K8 | Vnn1 | Pantetheinase [VNN1] | 1.89 | 0.0000 | 2.29 | 0.0000 |
| O35728 | Cyp4a14 | Cytochrome P450 4A14 [CP4AE] | 1.93 | 0.0000 | 2.28 | 0.0052 |
| Q9DBM2 | Ehhadh | Peroxisomal bifunctional enzyme [ECHP] | 2.21 | 0.0000 | 3.18 | 0.0000 |
| Q8VCH0 | Acaa1b | 3-ketoacyl-CoA thiolase B, peroxisomal [THIKB] | 2.72 | 0.0000 | 2.75 | 0.0000 |
| | | Down-Regulated | | | | |
| P58710 | Gulo | L-gulonolactone oxidase [GGLO] | 0.69 | 0.0002 | 0.55 | 0.0016 |
| P14246 | Slc2a2 | Solute carrier family 2, facilitated glucose transporter member 2 [GTR2] | 0.71 | 0.0018 | 0.70 | 0.0020 |
| Q00623 | Apoa1 | Apolipoprotein A-I [APOA1] | 0.75 | 0.0007 | 0.77 | 0.0064 |


dx.doi.org/10.1021/pr500641b | *J. Proteome Res.* XXXX, XXX, XXX−XXX

**Table 1. continued**

| accession | gene name | protein name | 1 mg/kg/d versus Ctrl | | 5 mg/kg/d versus Ctrl | |
|---|---|---|---|---|---|---|
| | | | fold change | *P* value | fold change | *P* value |
| | | Down-Regulated | | | | |
| P46656 | Fdx1 | Adrenodoxin, mitochondrial [ADX] | 0.76 | 0.0196 | 0.61 | 0.0000 |
| P56657 | Cyp2c40 | Cytochrome P450 2C40 [CP240] | 0.77 | 0.0227 | 0.62 | 0.0003 |
| P51885 | Lum | Lumican [LUM] | 0.77 | 0.0262 | 0.80 | 0.0226 |
| Q9WU79 | Prodh | Proline dehydrogenase 1, mitochondrial [PROD] | 0.77 | 0.0000 | 0.82 | 0.0044 |
| P16460 | Ass1 | Argininosuccinate synthase [ASSY] | 0.78 | 0.0004 | 0.69 | 0.0000 |
| Q8K0E8 | Fgb | Fibrinogen $\beta$ chain [FIBB] | 0.78 | 0.0164 | 0.65 | 0.0010 |
| Q8C196 | Cps1 | Carbamoyl-phosphate synthase [ammonia], mitochondrial [CPSM] | 0.80 | 0.0000 | 0.67 | 0.0000 |
| P53657 | Pklr | Pyruvate kinase isozymes R/L [KPYR] | 0.80 | 0.0009 | 0.74 | 0.0007 |
| Q9DBG1 | Cyp27a1 | Sterol 26-hydroxylase, mitochondrial [CP27A] | 0.82 | 0.0019 | 0.64 | 0.0009 |

[a]When the ratio of a protein between treatment and the control was ≥1.2 or ≤0.83 (and $P < 0.05$) in both of the duplicated experiments, the protein was considered to be altered significantly. All the fold change data are from one representative result of the duplicated experiments.

**Table 2. Altered miRNAs after PFNA Exposure[a,b]**

| mature miRNAs | | 1 mg/kg/d versus Ctrl | | 5 mg/kg/d versus Ctrl | |
|---|---|---|---|---|---|
| name | accession | fold change | *P* value | fold change | *P* value |
| | | Up-Regulated | | | |
| miR-34a | MIMAT0000542 | 2.76 | 0.0125 | 9.05 | 0.0011 |
| miR-1897-5p | MIMAT0007864 | | | 8.06 | 0.0281 |
| miR-107 | MIMAT0000647 | | | 2.10 | 0.0002 |
| miR-93 | MIMAT0000540 | | | 2.04 | 0.0004 |
| miR-152 | MIMAT0000162 | | | 2.07 | 0.0036 |
| miR-378 | MIMAT0003151 | | | 2.71 | 0.0051 |
| miR-96 | MIMAT0000541 | | | 6.82 | 0.0144 |
| miR-200c | MIMAT0000657 | | | 5.91 | 0.0193 |
| miR-296-5p | MIMAT0000374 | | | 3.54 | 0.0426 |
| miR-705 | MIMAT0003495 | | | 11.73 | 0.0004 |
| miR-378* | MIMAT0000742 | | | 2.21 | 0.0002 |
| miR-877 | MIMAT0004861 | | | 23.19 | 0.0021 |
| miR-185 | MIMAT0000214 | | | 2.03 | 0.0006 |
| miR-18a | MIMAT0000528 | | | 5.85 | 0.0048 |
| miR-669f | MIMAT0005839 | | | 5.68 | 0.0006 |
| miR-331-3p | MIMAT0000571 | | | 2.17 | 0.0003 |
| | | Down-Regulated | | | |
| miR-362-3p | MIMAT0004684 | −2.00 | 0.0206 | −2.81 | 0.0060 |
| miR-338-3p | MIMAT0000582 | −2.25 | 0.0324 | −3.05 | 0.0097 |
| miR-203 | MIMAT0000236 | | | −6.34 | 0.0029 |
| miR-455 | MIMAT0003742 | | | −5.67 | 0.0007 |
| miR-144 | MIMAT0000156 | | | −2.26 | 0.0201 |
| miR-100 | MIMAT0000655 | | | −2.34 | 0.0002 |
| miR-31* | MIMAT0004634 | | | −2.82 | 0.0019 |
| miR-7a | MIMAT0000677 | | | −2.49 | 0.0036 |
| miR-99a | MIMAT0000131 | | | −2.74 | 0.0011 |
| miR-130a | MIMAT0000141 | | | −2.57 | 0.0094 |
| miR-193 | MIMAT0000223 | | | −2.25 | 0.0037 |
| miR-142-3p | MIMAT0000155 | | | −2.28 | 0.0174 |
| miR-200a | MIMAT0000519 | | | −2.42 | 0.0362 |
| miR-342-3p | MIMAT0000590 | | | −5.02 | 0.0478 |

[a]Fold change of at least 2, $P < 0.05$. [b]Liver tissues from two individual mice in the same group were pooled into one sample, and hepatic total RNA from three pooled samples in each group were used for the miRNA assay.

(Lpl) (Figure 2B). The hepatic mRNA levels of SREBP targets, including mitochondrial hydroxymethylglutaryl-CoA synthase (Hmgcs2), farnesyl-diphosphate farnesyltransferase 1 (Fdft1), 3-hydroxy-3-methylglutaryl Coenzyme A reductase (Hmgcr), and low density lipoprotein receptor (Ldlr), which are all involved in the generation of cholesterol, were increased in the 1 mg/kg/d PFNA treatment group compared with the control (Figure 2C).

## iTRAQ Identified Proteins

To explore the global effect of PFNA on protein profiles, iTRAQ was carried out. We found that 108 (80 up-regulated, 28 down-regulated) and 342 hepatic proteins (179 up-regulated, 163 down-regulated) exhibited statistically significant


dx.doi.org/10.1021/pr500641b | J. Proteome Res. XXXX, XXX, XXX−XXX

changes (at least a 1.2-fold alteration and $P < 0.05$) in the 1 and 5 mg/kg/d PFNA treatment groups, respectively (details are shown in Supporting Information Table S4 and S5, respectively). Sixty-six proteins (54 up-regulated, 12 down-regulated) significantly changed in both of the two treatment groups (Table 1). Among the 54 up-regulated proteins, the GO category analysis indicated that most were involved in lipid metabolism processes (31 proteins), including peroxisomal 3-ketoacyl-CoA thiolase A (Acaa1a), mitochondrial medium-chain specific acyl-CoA dehydrogenase (Acadm), acyl-coenzyme A thioesterase 1 (Acot1), Acot2, Acot4, Acot8, Acox1, Acsl1, Acsl5, perilipin-2 (Adfp), retinal dehydrogenase 1 (Aldh1a1), catalase (Cat), platelet glycoprotein 4 (Cd36), carnitine O-acetyltransferase (Crat), Cyp4a10, Cyp4a12a, Cyp4a14, acyl-CoA-binding protein (Dbi), mitochondrial enoyl-CoA delta isomerase 1 (Dci), peroxisomal bifunctional enzyme (Ehhadh), fatty acid-binding protein 1 (Fabp1), 2-hydroxyacyl-CoA lyase 1 (Hacl1), mitochondrial trifunctional enzyme subunit $\alpha$ and $\beta$ (Hadha and Hadhb), Hmgcs2, estradiol 17-$\beta$-dehydrogenase 11 (Hsd17b11), peroxisomal multifunctional enzyme type 2 (Hsd17b4), hydroxysteroid dehydrogenase-like protein 2 (Hsdl2), Me1, monoglyceride lipase (Mgll), and phosphatidylcholine transfer protein (Pctp). Many of these up-regulated proteins are target genes of transcription factors PPAR $\alpha$ and SREBPs. Among these altered proteins, the mRNA levels of PPAR $\alpha$ targets: Acox1 and Cyp4a10, and SREBPs targets: Acsl1, Hmycs2 and Me1, were also found to be up-regulated in at least one of the three treatment groups by qPCR assay in Figure 2. Only 12 protein were down-regulated in both 1 and 5 mg/kg/d PFNA treatment groups, such as extracellular matrix structural proteins, lumican (Lum), fibrinogen $\beta$ chain (Fgb), saccharide metabolic proteins, and solute carrier family 2 (facilitated glucose transporter) member 2 (Slc2a2). No dominant GO category was presented in these down-regulated proteins.

### Effect of PFNA on Hepatic miRNA Levels

To gain insight into hepatic miRNAs response and their potential roles in PFNA treatment mice, the overall hepatic expression of miRNAs in mice treated with PFNA was investigated using Agilent miRNA microarray. The expression of all miRNAs after treatment is shown as volcano plots in Supporting Information Figure S2. A 2-fold and $P < 0.05$ threshold was set, and the results indicated that 1 mg/kg/d PFNA treatment for 14 days altered three miRNAs (down-regulated miR-338-3p and miR-362-3p, and up-regulated miR-34a) in mice livers (Table 2). Thirty altered miRNAs (14 down-regulated and 16 up-regulated) were identified in the 5 mg/kg/d PFNA treatment group, which included the three miRNAs altered by 1 mg/kg/d PFNA treatment. Thus, these three miRNAs may be more sensitive than others following PFNA exposure. Of the changed miRNAs, six miRNAs (miR-34a, miR-200c, miR-96, miR-18a, miR-342-3p, and miR-338-3p), which showed relatively higher fold change and whose sequences are conserved among mouse and human species, were selected and their alterations were further confirmed by TaqMan qPCR (Figure 3).

### Identification of miRNA Targets

To explore the potential involvement of altered miRNAs in the regulation of proteins in mice liver after PFNA treatment, we used the online database StarBase 2.0 to search for targets of the three miRNAs (miR-34a, miR-362-3p, and miR-338-3p) among the sixty-eight proteins (these miRNA and proteins

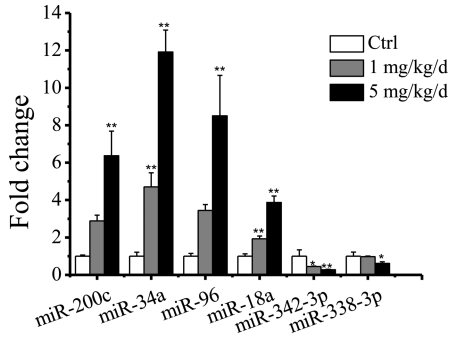


**Figure 3.** Validation of hepatic miRNA alteration. Abundance of six miRNAs was measured using TaqMan qPCR. U6 snRNA was chosen as an internal control for normalization. Differences were evaluated using one-way ANOVA followed by Fisher's least significant difference test. Error bars represent standard error (SE) ($n = 6$). * $P < 0.05$ versus control, ** $P < 0.01$ versus control.

were changed in both 1 and 5 mg/kg/d PFNA treatments). However, no potential miRNA-mRNA interaction was obtained. By further searching for targets of the 30 miRNAs among the three hundred and sixty-four proteins, which were changed in the highest dose of PFNA treatments groups compared with control, we found some proteins in the iTRAQ assay were potential targets of the altered miRNAs (Supporting Information Table S6).

The target identification work was not confined to proteins in the iTRAQ assay results. Several genes, which were not identified by iTRAQ after PFNA treatment but suggested by online prediction tools, were also included. The 3′ UTRs of Ldha and Fut8 mRNAs contained the complementary sequence to seed sites of miR-34a (Supporting Information Figure S3A, S3B), implying that Ldha and Fut8 were targets of miR-34a. After cotransfection with miR-34a mimic, decreases in firefly luciferase activity were observed in psiCHECK-2-Ldha and psiCHECK-2-Fut8 transfected HepG2 cells compared with psiCHECK-2 vector transfected cells (Figure 4A). Validation of these targets was further carried out by qPCR (Figure 4B) and Western blot analysis (Figure 4C), the results of which supported that Ldha and Fut8 were targets of miR-34a.

## DISCUSSION

Accumulated evidence has shown that the PPAR $\alpha$ agonistic mode of action is involved in the induction of hepatomegaly and peroxisomal $\beta$-oxidation observed in rodent bioassays with PFASs, such as PFOS and PFOA.[17,18,28] Moreover, in our study, prominent hepatomegaly and perturbation of lipid metabolism were observed in mice treated with PFNA. The mean serum PFNA concentration (11.5 $\mu$g/mL) in 0.2 mg/kg/d PFNA treatment animals is about 1000-fold the average levels of PFOA found in general human populations, and 100-fold their highest level of serum PFOS.[7] In the low-dose PFNA treated animals, we did not find alterations in most of the biochemical parameters' detection, including in the serum lipid and cholesterol levels, liver transaminase and TG and cholesterol levels. The only observable effect in animals after 0.2 mg/kg/d PFNA treatment was an increase in liver weight, indicating that liver weight was sensitive to PFNA. Studies showed that kinds of PFASs were associated with liver enlargement in rodents and nonhuman primates.[17] PPAR $\alpha$ influences lipid catabolism through direct transcriptional control of genes involved in peroxisomal and mitochondrial


dx.doi.org/10.1021/pr500641b | J. Proteome Res. XXXX, XXX, XXX−XXX

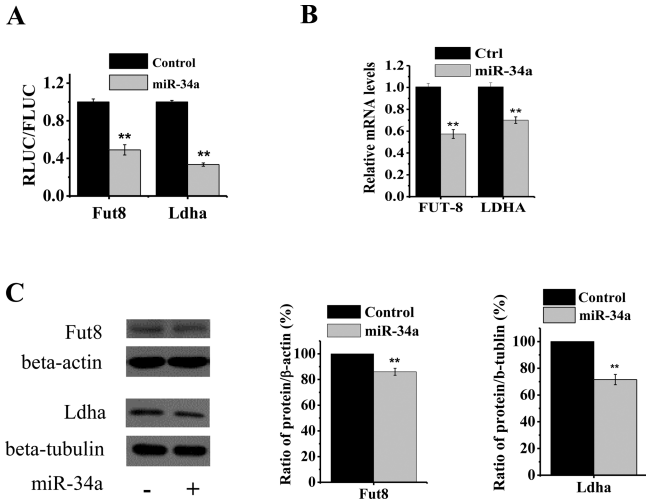


**Figure 4.** Potential miRNA targets identification. (A) Luciferase assay results for lactate dehydrogenase A (Ldha) and fucosyltransferase 8 (Fut8). Potential binding regions with miR-34a seeding sequence in 3′ UTR of Ldha and Fut8 were inserted into psiCHECK-2, the vectors were then cotransfected with miR-34a mimics into HepG2 cells, and luciferase assays were performed 48 h later. (B) qPCR and (C) Western blot results for the two genes 48 h after transfection. Differences were evaluated using Student's *t*-test. Error bars represent standard error (SE) ($n$ = 6). * $P$ < 0.05 versus control, ** $P$ < 0.01 versus control.

$\beta$-oxidation pathways, fatty acid uptake, triglyceride catabolism, and lipoprotein assembly and transport.[29−31] Transcriptional regulation by PPAR $\alpha$ is achieved by its direct binding to specific nucleotidic sequences known as peroxisome proliferator response elements (PPREs), which are present in the promoter region of target genes.[32] In the present study, iTRAQ assay identified that up-regulated proteins dominantly participated in lipid metabolism processes, with many involved in the PPAR $\alpha$ pathway, such as Acaa1a, Acox1, Acadm, Acot, Acsl1, Acsl5, Cd36, Cyp4a10, Cyp4a14, Dbi, Ehhadh, Fabp1, and Hmgcs2. In the iTRAQ assay study of hepatic protein alterations after PFOS exposure by Tan and his colleagues, the most dominant altered proteins were proteins related to lipid metabolism. Especially proteins involved in peroxisomal $\beta$-oxidation were significantly up-regulated, including Slc27a2, Ehhadh, Acox1, and Acaa1a.[33] All of the four proteins were found to be increased at least in one of the two PFNA treatment groups by our iTRAQ assay. In a genomic dissection of the hepatic transcript profile in liver using PPAR $\alpha$ deleted mouse, Rosen and his colleagues found that 85% genes altered by PFOA were through PPAR $\alpha$.[34] The PPAR $\alpha$ agonistic activity of PFNA was also confirmed by the increase in hepatic mRNA levels in PPAR $\alpha$ target genes in the PFNA treated mice, including Acox1 and Cyp4a10, the protein levels of which were identified as up-regulated by iTRAQ in the present study. Another gene, Mlycd, which catalyzes malonyl-CoA decarboxylation, were identified as PPAR $\alpha$ target[35] and increased after PFNA treatment. The mRNA levels of two apolipoproteins, Apoa4 and Apoc3a, which are up- and down-regulated by PPAR $\alpha$, respectively,[36,37] showed similar tendencies which were predicted. Fatty acid omega-hydroxylation was governed by the subfamily of Cyp4a enzymes.[38] In our study, Cyp4a10, a Cyp4a family member, was also significantly up-regulated after PFNA treatment in both mRNA and protein levels. The above results support that the PPAR $\alpha$ agonistic effect of PFNA resulted in the decrease in animal weight, as well as serum TG and TCHO levels in the highest PFNA treatment group.

Although strong evidence supports the idea that some PFASs induce liver toxicity via a PPAR $\alpha$ agonistic mode in rodents, treatment with PFASs may result in changes mediated by other pathways. As for hepatic TG and TCHO levels, the significant increases in the low and median dose groups cannot be explained by the PPAR $\alpha$ agonistic mode alone. In the iTRAQ assay, many proteins involved in fatty acid and cholesterol biosynthesis were also up-regulated, such as Acsl1, Hmgcs2, and Me1. Belonging to the basic helix−loop−helix−leucine zipper (bHLH-Zip) family of transcription factors, SREBPs play a central role in controlling the transcription of genes involved in cholesterol, fatty acids, and triglycerides generation.[39−41] Two SREBP genes (SREBP1 and SREBP2) have been found, which transcribe three transcripts (SREBP1a, SREBP1c, and SREBP2), with SREBP1 dominant in liver.[42] The hepatic mRNAs for fatty acid and triglyceride synthesis genes, including Me1, Acaca, Fasn, Gpam, Scd1, Acsl1, and Elovl6, all increased after PFNA treatment, especially in the median dose group. Similarly, the mRNA levels of genes involved in the generation of cholesterol, such as Hmgcs2, Fdft1, Hmgcr, and Ldlr, also showed the same increasing trend as each other. In addition, the median PFNA dose also up-regulated the mRNA level of Lpl, which is a fatty acid uptake enzyme modulated transcriptionally by SREBPs.[43] The above results indicated that fatty acid and cholesterol biosynthetic pathways were activated after PFNA treatment. It may be the more dominant activation of fatty acid and cholesterol biosynthetic pathways than that of lipolysis procession at the median PFNA dose that promoted the net intracellular accumulation of hepatic cholesterol/triglyceride.

MiRNAs are 21−23 nucleotide RNA molecules that post-transcriptionally repress target gene expression in animals.[44] The most general feature of miRNA regulation is the recognition of sequence motifs complementary to the seed region (nucleotides 2−7 of the miRNA) in the 3′ UTR of target mRNAs.[45] Treatment with PFNA altered hepatic miRNA expression profiles in mice significantly, which implied that complicated effects might be exerted through these noncoding RNA molecules. Several PFNA response miRNAs, including miR-34a, miR-107, miR-93, miR-378, miR-200c, miR-203, miR-99a, and miR-100, also showed similar alteration tendencies after being induced by WY-14643, a kind of peroxisome proliferator.[46] These results implied that these miRNAs might be involved in PPAR agonist-induced biological and pathological processes in the liver, although probably indirectly. Among the miRNAs, miR-34a and miR-200c levels have been found to be significantly altered under hepatic injury or disease conditions.[47,48] Ladeiro and his colleagues found that the hepatic level of miR-200c decreased in patients with benign tumors, whereas the level of hepatic miR-200c increased in patients with hepatocellular carcinoma.[48] The potential function of hepatic miR-200c in disease conditions needs elucidated in future. Huang and his colleagues studied PFOA-induced apoptosis in human hepatic cell L-02 and suggested that p53-dependent mitochondrial pathway played an important role in this process.[49] Although no alteration of pro-apoptotic proteins was detected in our iTRAQ results, we found a great increase in the level of hepatic miR-34a after PFNA treatment. Accumulating evidence suggests that miR-34a acts as a key mediator of p53 tumor suppression and mediates induction of apoptosis, cell cycle arrest, and senescence.[50,51]


dx.doi.org/10.1021/pr500641b | J. Proteome Res. XXXX, XXX, XXX−XXX

Due to the laborious nature of experiments and the absence of direct high-throughput experimental approaches, computational methods have been used to predict miRNA targets.[52] These computational algorithms are most commonly based on 5′ seed matches; moreover, to increase accuracy, other features such as evolutionary conservation, secondary structure of target transcripts, and nucleotide composition of target sequences are often included.[45,53] Online database searching results showed that Ldha and Fut8 were potential targets of miR-34a. Using luciferase activity assay, qPCR, and Western blot analysis, we confirmed that Ldha and Fut8 were down-regulated by miR-34a. It is well known that Ldha catalyzes the interconversion of pyruvate and lactate with concomitant interconversion of NADH and NAD(+). Our results implied that by post-transcriptionally regulating Ldha, miR-34a might participate in the gluconeogenesis and glycolysis pathways. In mammals, Fut8 catalyzes the transfer of fucose residue to N-linked oligosaccharides on glycoproteins via an $\alpha$ 1,6-linkage to form core fucosylation. Core fucosylated N-glycans are widely distributed in a variety of glycoproteins and are altered under certain hepatic pathological conditions, including hepatocarcinogenesis.[54] The presence of core fucosylation of $\alpha$-fetoprotein is a well-known tumor marker for hepatocellular carcinoma.[55] The results of the studies mentioned above implied that miR-34a might also be involved in cell cycle regulation and apoptosis through Fut8. Online database results showed that less changed proteins in iTRAQ assay were potential targets of the altered miRNAs, which was likely due to the moderate character of the repression effect for miRNAs.[56]

## CONCLUSION

Administration of PFNA led to hepatic lesions, including hepatomegaly and perturbation of lipid metabolism and transport. Such hepatic effects executed by PFNA cannot simply be explained by the PPAR $\alpha$ agonistic mode of action. The activation of fatty acid and cholesterol biosynthetic pathways were involved in the process. MiRNAs, such as miR-34a and miR-200c, might also play important roles in the regulation of post-translational protein repression after PFNA treatment.

## ASSOCIATED CONTENT

### Supporting Information

Supplementary Figure S1 displays the PFNA content in mouse liver (A) and serum (B) after treatment. Supplementary Figure S2 displays the volcano plots of miRNAs expression in PFNA treated mice liver tissues. Supplementary Figure S3 shows the potential binding sites of target genes. Quality control for PFNA concentration detection is shown in Supplementary Table S1. Gene-specific primers used in qPCR and 3′ UTR psiCHECK-2 vector preparation are shown in Supplementary Table S2 and S3, respectively. Significantly altered proteins in 1 and 5 mg/kg/d PFNA treatment groups are listed in Supplementary Table S4 and S5, respectively. Potential regulations of altered miRNAs in proteins changed in iTRAQ assay are listed in Supplementary Table S6. This material is available free of charge via the Internet at http://pubs.acs.org.

## AUTHOR INFORMATION

### Corresponding Author

*E-mail: daijy@ioz.ac.cn. Tel. +86-10-6480-7185.

### Notes

The authors declare no competing financial interest.

## ACKNOWLEDGMENTS

This work was supported by the Strategic Priority Research Program of the Chinese Academy of Sciences (XDB14040202) and the National Natural Science Foundation of China (grants No. 31320103915, 21277143, and 31025006).

## ABBREVIATIONS

Alanine transaminase, ALT; Aspartate aminotransferase, AST; Basic helix−loop−helix−leucine zipper, bHLH-Zip; Fucosyltransferase 8, Fut8; Gene Ontology, GO; High-performance liquid chromatography-tandem mass spectrometry, HPLC−MS/MS; Isobaric tags for relative and absolute quantitation, iTRAQ; Lactate dehydrogenase, Ldha; Limit of quantifications, LOQs; Long-chain-fatty-acid-CoA ligase1, Acsl1; Low-density lipoprotein cholesterol, LDL-C; MicroRNA, miRNA; Perfluoroalkyl chemical, PFAS; Perfluorocarboxylic acid, PFCA; Perfluorononanoic acid, PFNA; Perfluorooctanesulfonate, PFOS; Perfluorooctanoic acid, PFOA; Peroxisome proliferator-activated receptors $\alpha$, PPAR $\alpha$; Peroxisome proliferator response element, PPRE; Quantitative PCR, qPCR; Sterol regulatory element-binding proteins, SREBPs; Total cholesterol, TCHO; Triglycerides, TG; Untranslated region, UTR

## REFERENCES

(1) Calafat, A. M.; Wong, L. Y.; Kuklenyik, Z.; Reidy, J. A.; Needham, L. L. Polyfluoroalkyl chemicals in the U.S. population: data from the National Health and Nutrition Examination Survey (NHANES) 2003−2004 and comparisons with NHANES 1999−2000. *Environ. Health Perspect.* **2007**, *115*, 1596−1602.

(2) Olsen, G. W.; Zobel, L. R. Assessment of lipid, hepatic, and thyroid parameters with serum perfluorooctanoate (PFOA) concentrations in fluorochemical production workers. *Int. Arch. Occup. Environ. Health* **2007**, *81*, 231−246.

(3) Kannan, K.; Corsolini, S.; Falandysz, J.; Fillmann, G.; Kumar, K. S.; Loganathan, B. G.; Mohd, M. A.; Olivero, J.; Van Wouwe, N.; Yang, J. H.; Aldoust, K. M. Perfluorooctanesulfonate and related fluorochemicals in human blood from several countries. *Environ. Sci. Technol.* **2004**, *38*, 4489−4495.

(4) Karrman, A.; Mueller, J. F.; van Bavel, B.; Harden, F.; Toms, L. M. L.; Lindstrom, G. Levels of 12 perfluorinated chemicals in pooled Australian serum, collected 2002−2003, in relation to age, gender, and region. *Environ. Sci. Technol.* **2006**, *40*, 3742−3748.

(5) Fromme, H.; Tittlemier, S. A.; Volkel, W.; Wilhelm, M.; Twardella, D. Perfluorinated compounds−exposure assessment for the general population in Western countries. *Int. J. Hyg. Environ. Health* **2009**, *212*, 239−270.

(6) Giesy, J.; Kannan, K. Global distribution of perfluorooctanoate sulfonate in wildlife. *Environ. Sci. Technol.* **2001**, *35*, 1339−1342.

(7) Lau, C.; Anitole, K.; Hodes, C.; Lai, D.; Pfahles-Hutchens, A.; Seed, J. Perfluoroalkyl acids: A review of monitoring and toxicological findings. *Toxicol. Sci.* **2007**, *99*, 366−394.

(8) So, M. K.; Yamashita, N.; Taniyasu, S.; Jiang, Q.; Giesy, J. P.; Chen, K.; Lam, P. K. Health risks in infants associated with exposure to perfluorinated compounds in human breast milk from Zhoushan, China. *Environ. Sci. Technol.* **2006**, *40*, 2924−2929.

(9) Jensen, A. A.; Leffers, H. Emerging endocrine disrupters: perfluoroalkylated substances. *Int. J. Androl.* **2008**, *31*, 161−169.

(10) Ishibashi, H.; Iwata, H.; Kim, E. Y.; Tao, L.; Kannan, K.; Amano, M.; Miyazaki, N.; Tanabe, S.; Batoev, V. B.; Petrov, E. A. Contamination and effects of perfluorochemicals in Baikal Seal (*Pusa sibirica*). 1. Residue level, tissue distribution, and temporal trend. *Environ. Sci. Technol.* **2008**, *42*, 2295−2301.

(11) Haug, L. S.; Thomsen, C.; Brantsaeter, A. L.; Kvalem, H. E.; Haugen, M.; Becher, G.; Alexander, J.; Meltzer, H. M.; Knutsen, H. K. Diet and particularly seafood are major sources of perfluorinated compounds in humans. *Environ. Int.* **2010**, *36*, 772−778.
(12) Jones, P.; Hu, W.; De Coen, W.; Newsted, J.; Giesy, J. Binding of perfluorinated fatty acids to serum proteins. *Environ. Toxicol. Chem.* **2003**, *22*, 2639−2649.
(13) Hundley, S.; Sarrif, A.; Kennedy, G. Absorption, distribution and excretion of ammonium perfluorooctanoate (APFO) after oral administration in various species. *Drug Chem. Toxicol.* **2006**, *29*, 137−145.
(14) Steenland, K.; Tinker, S.; Frisbee, S.; Ducatman, A.; Vaccarino, V. Association of perfluorooctanoic acid and perfluorooctane sulfonate with serum lipids among adults living near a chemical plant. *Am. J. Epidemiol.* **2009**, *170*, 1268−1278.
(15) Frisbee, S. J.; Shankar, A.; Knox, S. S.; Steenland, K.; Savitz, D. A.; Fletcher, T.; Ducatman, A. M. Perfluorooctanoic acid, perfluorooctanesulfonate, and serum lipids in children and adolescents: results from the C8 Health Project. *Arch. Pediatr. Adolesc. Med.* **2010**, *164*, 860−869.
(16) Kudo, N.; Kawashima, Y. Toxicity and toxicokinetics of perfluorooctanoic acid in humans and animals. *J. Toxicol. Sci.* **2003**, *28*, 49−57.
(17) Kennedy, G. L., Jr; Butenhoff, J. L.; Olsen, G. W.; O'Connor, J. C.; Seacat, A. M.; Perkins, R. G.; Biegel, L. B.; Murphy, S. R.; Farrar, D. G. The toxicology of perfluorooctanoate. *Crit. Rev. Toxicol.* **2004**, *34*, 351−384.
(18) Abbott, B. D.; Wolf, C. J.; Schmid, J. E.; Das, K. P.; Zehr, R. D.; Helfant, L.; Nakayama, S.; Lindstrom, A. B.; Strynar, M. J.; Lau, C. Perfluorooctanoic acid induced developmental toxicity in the mouse is dependent on expression of peroxisome proliferator activated receptor-$\alpha$. *Toxicol. Sci.* **2007**, *98*, 571−581.
(19) Andersen, M. E.; Butenhoff, J. L.; Chang, S. C.; Farrar, D. G.; Kennedy, G. L., Jr.; Lau, C.; Olsen, G. W.; Seed, J.; Wallace, K. B. Perfluoroalkyl acids and related chemistries-toxicokinetics and modes of action. *Toxicol. Sci.* **2008**, *102*, 3−14.
(20) Bartel, D. P. MicroRNAs: genomics, biogenesis, mechanism, and function. *Cell* **2004**, *116*, 281−297.
(21) Wahid, F.; Shehzad, A.; Khan, T.; Kim, Y. Y. MicroRNAs: synthesis, mechanism, function, and recent clinical trials. *Biochim. Biophys. Acta* **2010**, *1803*, 1231−1243.
(22) Wetmore, B. A.; Merrick, B. A. Toxicoproteomics: proteomics applied to toxicology and pathology. *Toxicol. Pathol.* **2004**, *32*, 619−642.
(23) Ross, P. L.; Huang, Y. N.; Marchese, J. N.; Williamson, B.; Parker, K.; Hattan, S.; Khainovski, N.; Pillai, S.; Dey, S.; Daniels, S.; Purkayastha, S.; Juhasz, P.; Martin, S.; Bartlet-Jones, M.; He, F.; Jacobson, A.; Pappin, D. J. Multiplexed protein quantitation in *Saccharomyces cerevisiae* using amine-reactive isobaric tagging reagents. *Mol. Cell. Proteomics* **2004**, *3*, 1154−1169.
(24) Livak, K. J.; Schmittgen, T. D. Analysis of relative gene expression data using real-time quantitative PCR and the 2(-Delta Delta C(T)) method. *Methods* **2001**, *25*, 402−408.
(25) Benjamini, Y.; Hochberg, Y. Controlling the false discovery rate: a practical and powerful approach to multiple testing. *J. R. Stat. Soc., B* **1995**, *57*, 289−300.
(26) Li, J. H.; Liu, S.; Zhou, H.; Qu, L. H.; Yang, J. H. starBase v2.0: decoding miRNA-ceRNA, miRNA-ncRNA and protein-RNA interaction networks from large-scale CLIP-Seq data. *Nucleic Acids Res.* **2014**, *42*, D92−D97.
(27) Yang, J. H.; Li, J. H.; Shao, P.; Zhou, H.; Chen, Y. Q.; Qu, L. H. starBase: a database for exploring microRNA-mRNA interaction maps from Argonaute CLIP-Seq and Degradome-Seq data. *Nucleic Acids Res.* **2011**, *39*, D202−D209.
(28) Cheung, C.; Akiyama, T. E.; Ward, J. M.; Nicol, C. J.; Feigenbaum, L.; Vinson, C.; Gonzalez, F. J. Diminished hepatocellular proliferation in mice humanized for the nuclear receptor peroxisome proliferator-activated receptor $\alpha$. *Cancer Res.* **2004**, *64*, 3849−3854.
(29) Lee, S. S.; Pineau, T.; Drago, J.; Lee, E. J.; Owens, J. W.; Kroetz, D. L.; Fernandez-Salguero, P. M.; Westphal, H.; Gonzalez, F. J. Targeted disruption of the $\alpha$ isoform of the peroxisome proliferator-activated receptor gene in mice results in abolishment of the pleiotropic effects of peroxisome proliferators. *Mol. Cell. Biol.* **1995**, *15*, 3012−3022.
(30) Aoyama, T.; Peters, J. M.; Iritani, N.; Nakajima, T.; Furihata, K.; Hashimoto, T.; Gonzalez, F. J. Altered constitutive expression of fatty acid-metabolizing enzymes in mice lacking the peroxisome proliferator-activated receptor $\alpha$ (PPAR$\alpha$). *J. Biol. Chem.* **1998**, *273*, 5678−5684.
(31) Kersten, S.; Desvergne, B.; Wahli, W. Roles of PPARs in health and disease. *Nature* **2000**, *405*, 421−424.
(32) IJpenberg, A.; Jeannin, E.; Wahli, W.; Desvergne, B. Polarity and specific sequence requirements of peroxisome proliferator-activated receptor (PPAR)/retinoid X receptor heterodimer binding to DNA. A functional analysis of the malic enzyme gene PPAR response element. *J. Biol. Chem.* **1997**, *272*, 20108−20117.
(33) Tan, F.; Jin, Y.; Liu, W.; Quan, X.; Chen, J.; Liang, Z. Global liver proteome analysis using iTRAQ labeling quantitative proteomic technology to reveal biomarkers in mice exposed to perfluorooctane sulfonate (PFOS). *Environ. Sci. Technol.* **2012**, *46*, 12170−12177.
(34) Rosen, M. B.; Lee, J. S.; Ren, H.; Vallanat, B.; Liu, J.; Waalkes, M. P.; Abbott, B. D.; Lau, C.; Corton, J. C. Toxicogenomic dissection of the perfluorooctanoic acid transcript profile in mouse liver: evidence for the involvement of nuclear receptors PPAR $\alpha$ and CAR. *Toxicol. Sci.* **2008**, *103*, 46−56.
(35) Lee, G. Y.; Kim, N. H.; Zhao, Z. S.; Cha, B. S.; Kim, Y. S. Peroxisomal-proliferator-activated receptor $\alpha$ activates transcription of the rat hepatic malonyl-CoA decarboxylase gene: a key regulation of malonyl-CoA level. *Biochem. J.* **2004**, *378*, 983−990.
(36) Staels, B.; Vu-Dac, N.; Kosykh, V. A.; Saladin, R.; Fruchart, J. C.; Dallongeville, J.; Auwerx, J. Fibrates downregulate apolipoprotein C-III expression independent of induction of peroxisomal acyl coenzyme A oxidase. A potential mechanism for the hypolipidemic action of fibrates. *J. Clin. Invest.* **1995**, *95*, 705−712.
(37) Nagasawa, M.; Akasaka, Y.; Ide, T.; Hara, T.; Kobayashi, N.; Utsumi, M.; Murakami, K. Highly sensitive upregulation of apolipoprotein A-IV by peroxisome proliferator-activated receptor $\alpha$ (PPAR$\alpha$) agonist in human hepatoma cells. *Biochem. Pharmacol.* **2007**, *74*, 1738−1746.
(38) Johnson, E. F.; Palmer, C. N.; Griffin, K. J.; Hsu, M. H. Role of the peroxisome proliferator-activated receptor in cytochrome P450 4A gene regulation. *FASEB J.* **1996**, *10*, 1241−1248.
(39) Lopez, J. M.; Bennett, M. K.; Sanchez, H. B.; Rosenfeld, J. M.; Osborne, T. F. Sterol regulation of acetyl CoA carboxylase: a mechanism for coordinate control of cellular lipid. *Proc. Natl. Acad. Sci. U.S.A.* **1996**, *93*, 1049−1053.
(40) Brown, M. S.; Goldstein, J. L. The SREBP pathway: regulation of cholesterol metabolism by proteolysis of a membrane-bound transcription factor. *Cell* **1997**, *89*, 331−340.
(41) Horton, J. D.; Shimomura, I. Sterol regulatory element-binding proteins: activators of cholesterol and fatty acid biosynthesis. *Curr. Opin. Lipidol.* **1999**, *10*, 143−150.
(42) Shimomura, I.; Shimano, H.; Horton, J. D.; Goldstein, J. L.; Brown, M. S. Differential expression of exons 1a and 1c in mRNAs for sterol regulatory element binding protein-1 in human and mouse organs and cultured cells. *J. Clin. Invest.* **1997**, *99*, 838−845.
(43) Schoonjans, K.; Gelman, L.; Haby, C.; Briggs, M.; Auwerx, J. Induction of LPL gene expression by sterols is mediated by a sterol regulatory element and is independent of the presence of multiple E boxes. *J. Mol. Biol.* **2000**, *304*, 323−334.
(44) Lee, R. C.; Feinbaum, R. L.; Ambros, V. The C. elegans heterochronic gene lin-4 encodes small RNAs with antisense complementarity to lin-14. *Cell* **1993**, *75*, 843−854.
(45) Lewis, B. P.; Shih, I. H.; Jones-Rhoades, M. W.; Bartel, D. P.; Burge, C. B. Prediction of mammalian microRNA targets. *Cell* **2003**, *115*, 787−798.

(46) Shah, Y. M.; Morimura, K.; Yang, Q.; Tanabe, T.; Takagi, M.; Gonzalez, F. J. Peroxisome proliferator-activated receptor $\alpha$ regulates a microRNA-mediated signaling cascade responsible for hepatocellular proliferation. *Mol. Cell. Biol.* **2007**, *27*, 4238−4247.
(47) Meng, F.; Glaser, S. S.; Francis, H.; Yang, F.; Han, Y.; Stokes, A.; Staloch, D.; McCarra, J.; Liu, J.; Venter, J.; Zhao, H.; Liu, X.; Francis, T.; Swendsen, S.; Liu, C. G.; Tsukamoto, H.; Alpini, G. Epigenetic regulation of miR-34a expression in alcoholic liver injury. *Am. J. Pathol.* **2012**, *181*, 804−817.
(48) Ladeiro, Y.; Couchy, G.; Balabaud, C.; Bioulac-Sage, P.; Pelletier, L.; Rebouissou, S.; Zucman-Rossi, J. MicroRNA profiling in hepatocellular tumors is associated with clinical features and oncogene/tumor suppressor gene mutations. *Hepatology* **2008**, *47*, 1955−1963.
(49) Huang, Q.; Zhang, J.; Martin, F. L.; Peng, S.; Tian, M.; Mu, X.; Shen, H. Perfluorooctanoic acid induces apoptosis through the p53-dependent mitochondrial pathway in human hepatic cells: a proteomic study. *Toxicol. Lett.* **2013**, *223*, 211−20.
(50) Bommer, G. T.; Gerin, I.; Feng, Y.; Kaczorowski, A. J.; Kuick, R.; Love, R. E.; Zhai, Y.; Giordano, T. J.; Qin, Z. S.; Moore, B. B.; MacDougald, O. A.; Cho, K. R.; Fearon, E. R. p53-mediated activation of miRNA34 candidate tumor-suppressor genes. *Curr. Biol.* **2007**, *17*, 1298−1307.
(51) He, L.; He, X.; Lim, L. P.; de Stanchina, E.; Xuan, Z.; Liang, Y.; Xue, W.; Zender, L.; Magnus, J.; Ridzon, D.; Jackson, A. L.; Linsley, P. S.; Chen, C.; Lowe, S. W.; Cleary, M. A.; Hannon, G. J. A microRNA component of the p53 tumour suppressor network. *Nature* **2007**, *447*, 1130−1134.
(52) Bartel, D. P. MicroRNAs: target recognition and regulatory functions. *Cell* **2009**, *136*, 215−233.
(53) Min, H.; Yoon, S. Got target? Computational methods for microRNA target prediction and their extension. *Exp. Mol. Med.* **2010**, *42*, 233−244.
(54) Hutchinson, W. L.; Du, M. Q.; Johnson, P. J.; Williams, R. Fucosyltransferases: differential plasma and tissue alterations in hepatocellular carcinoma and cirrhosis. *Hepatology* **1991**, *13*, 683−688.
(55) Sato, Y.; Nakata, K.; Kato, Y.; Shima, M.; Ishii, N.; Koji, T.; Taketa, K.; Endo, Y.; Nagataki, S. Early recognition of hepatocellular carcinoma based on altered profiles of $\alpha$-fetoprotein. *N. Engl. J. Med.* **1993**, *328*, 1802−1806.
(56) Baek, D.; Villen, J.; Shin, C.; Camargo, F. D.; Gygi, S. P.; Bartel, D. P. The impact of microRNAs on protein output. *Nature* **2008**, *455*, 64−71.